CONF-8808116--2

DE89 005878

The submitted manuscript has been authored by a contractor of the U. S. Government under contract No. W-31-109-ENG-38. Accordingly, the U. S. Government retains a nonexclusive, royalty-free license to publish or reproduce the published form of this contribution, or allow others to do so, for U. S. Government purposes.

FUSION-FISSION IN LIGHT NUCLEAR SYSTEMS

S.J. Sanders

Argonne National Laboratory, Argonne, Illinois 60439 U.S.A.

ABSTRACT The fission process, which has been largely ignored for reactions involving light nuclear systems, will be shown to play a significant role in the $^{32}S+^{24}Mg$ reaction at energies greater than about 1 1/2 times the Coulomb barrier energy. The magnitude of the fusion-fission cross section and its fragment mass dependence are found to be consistent with newer estimates of the fission barriers in lighter systems. The presence of the fission mechanism has significance for understanding the limitation to fusion at higher energies and has implications for comparisons of model calculations of evaporation-residue and associated light-particle yields with experiment.

1. INTRODUCTION

The fusion process in light nuclear systems (A<80) is generally viewed in terms of the formation of a compound nucleus which subsequently decays by light-particle emission (n, p, α). It is only in heavier systems that fission decay is seen to compete with light-particle emission, with its absence in lighter systems taken as an indication of the predicted high fission barriers for these masses. In this talk I would like to suggest that this picture may be too simplistic and that fission is indeed a significant process even towards the beginning of the periodic table—one which needs to be investigated if we are to develop an understanding of the dynamics of reactions involving these systems at higher energies.

Fission, for all masses, is one of the more dramatic of nuclear processes as it involves the large-scale breakup of the nucleus. Its study teaches us about nuclear dynamics and the structure of nuclei which are fleetingly created under extreme conditions of temperature and spin. An obvious connection exists in heavy-ion reactions between fission and the time-reversed process of fusion, with the absence of a fission barrier at higher spins possibly being responsible for the limitation of fusion seen at higher energies. Detailed studies of the fission process can be used to test calculations of the macroscopic nuclear potential energy surface. This is of topical interest because of the newer calculations which extend the

MASTER

rotating liquid drop model by incorporating diffuse-surface and finite-nuclear-range effects[1] (corrections which are greatest for lower masses).

For the fission of light systems we can expect significant differences in behavior to that observed with heavier masses stemming in part from differences in the mass-asymmetry dependence of the saddle-point energies, but also from the extended nature of the saddle-point configuration and the near degeneracy of the saddle and scission configurations. The latter differences account for why we would not expect an "extra push" to be needed for the fusion of these systems. Heavier systems are stable against asymmetric decay and, at least at energies where shell corrections to the macroscopic energy surface can be ignored, symmetric fission is both predicted and observed. For lighter masses, below the Businaro-Gallone point, the asymmetry dependent fission barriers favor the asymmetric breakup of the compound nucleus, a feature which has been established in the fission decay of ^{110}In as populated through the ^{3}He $+^{nat}$Ag reaction[2]. The occurrence of asymmetric decay suggests that perhaps the best way to study fission in these light systems is by starting with a mass symmetric entrance channels, and then looking for the fission yield in the asymmetric mass channels. Deep-inelastic processes, which would be expected to peak near the entrance-channel mass partition, are also discriminated against in this manner.

Fission-like yields have been observed in a number of studies of reactions reaching the mass A~50-60 region[3-7], but in general these studies have either been at sufficiently high an energy that processes involving incomplete momentum transfer complicate the analysis, or the fission yields are only observed in singles where it is not possible to correct for secondary light-particle emission from the fission fragments.

In this talk I will first discuss a coincidence measurement of the fission yields in the ^{32}S+^{24}Mg reaction[8,9], showing that the breakup of the ^{56}Ni compound nucleus does favor the more mass asymmetric fission channels. This result confirms an earlier, singles measurement of the fission-like yields from the ^{16}O+^{40}Ca reaction[5] (reaching the same ^{56}Ni compound nucleus) where asymmetric fission was suggested, but where only the more symmetric fission yields could be identified. I will then show that the observed behavior can be understood within the context of

statistical decay of the compound nucleus using newer estimates of the macroscopic energy surface.

2. EXPERIMENTAL RESULTS

To establish the full mass dependence of the fission yields from the $^{32}S+^{24}Mg$ system, both reaction fragments were detected in coincidence at $E_{lab}(^{32}S)$ = 121.1 and 141.9 MeV.[8,9] With the coincidence measurement, it is possible not only to determine clearly the full mass dependence of the observed binary reaction fragments, but also to deduce the primary mass distribution prior to secondary light particle evaporation from these fragments. Five Si(Surface Barrier) detectors were located on one side of the beam covering angles between 8° and 48°. By measuring the particle energy and time-of-flight with respect to the ATLAS rf timing signal, it was possible to determine the velocities and masses of the detected fragments. On the opposite side of the beam were located two 8 cm x 9 cm position-sensitive, multiwire proportional counters (MWPC) from which the velocity of the recoiling fragments could be determined. In two settings the proportional detectors covered the full angular range between 6° and 96°. In addition an array of seven, closely spaced, rectangular Si (SB) detectors were located behind the rear MWPC which could be used for ^{8}Be identification through the detection of the coincident α-particles from the ^{8}Be decay.

The fission yields are characterized by full energy damping (i.e. angle-independent total kinetic energies) and angular distributions which have a $1/\sin\theta$ dependence[9], as expected for isotropic decay in the plane perpendicular to the spin vector. The measured fission folding angles are found to be centered at the angles corresponding to full momentum transfer. In this regard, these results do not support the analysis of Moro *et al.*[7] where fully-energy-damped yields for the $^{30}Si+^{30}Si$ reaction at $E_{lab}(^{28}Si)$=120 MeV are interpreted in terms of an incomplete fusion mechanism. In that measurement, however, the folding-angle distributions were not measured.

From the measurement of the two fragment velocities it is possible to deduce the primary-mass distribution. If no secondary light particles are emitted, momentum conservation gives for the masses (labeled 1 and 2) $M_{1(2)}$ of the reaction products

$$M_{1(2)} = M_{total} \frac{V_{2(1)}^{c.m.}}{V_1^{c.m.} + V_2^{c.m.}} ,$$

where the velocities are in the compound-nucleus center-of-mass system (two-body kinematics are assumed). The effect of light-particle evaporation is to broaden the mass distributions derived from the velocity measurements, but, under reasonable assumptions concerning the light-particle decay, the average values of the deduced masses will not be changed.

The bold histograms in Fig. 1 show the primary mass distributions deduced from the coincidence measurement for different observed masses in the Si surface barrier detectors with $12 \leq A^{observed} \leq 28$. These data were obtained at $E_{c.m.}=60.8$ MeV and at $\theta_{lab}=28^o$. For the lower observed masses, $A^{observed}=12$, 16, and 20, the deduced primary, pre-evaporation mass distributions are found to be symmetric and centered with $A^{pre\text{-}evaporation} = A^{observed}$. This indicates that the mass identified fragments arise from the primary decay of the ^{56}Ni compound system. The broadening of the distributions is understood in terms of the statistical emission of light particles from the recoiling fragment prior to its detection in the MWPC. For the heavier observed masses there is a clear indication that a fraction of the events correspond to cases where the detected fragment has emitted of a light particle.

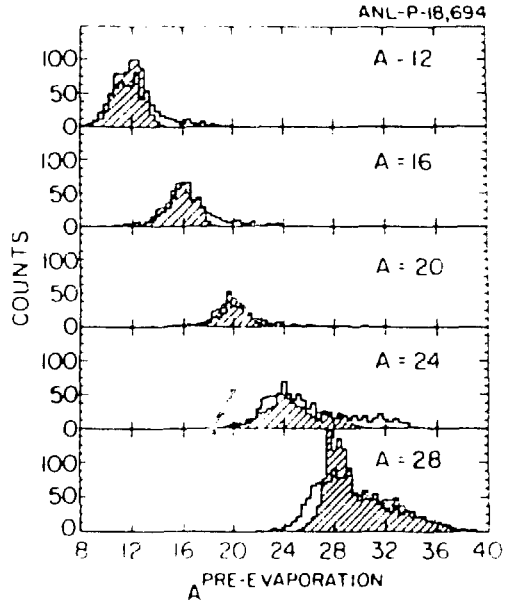

Figure 1. Pre-evaporation mass distributions derived from the measured fragment velocities for different regions of the observed mass spectrum at $\theta_{lab}=28.1^o$ (bold histograms) and the corresponding mass spectra obtained from the Monte-Carlo simulation described in the text (shaded histograms).

These distributions, along with the observed velocity spectra, were simulated using the Monte Carlo statistical evaporation code LILITA[10]. From this simulation it was possible to determine the pre-evaporation mass distributions at the two beam energies. The procedure used was to iterate on an assumed primary mass distribution for the binary decay and try to obtain the best fit to the observed velocity and mass distributions. The lighter, cross-hatched histograms in Fig. 1 indicate the results of this LILITA simulation for the pre-evaporation mass spectra leading to specific final masses. Fig. 2 shows both the observed mass distributions and the corresponding distributions corrected for light-particle evaporation.

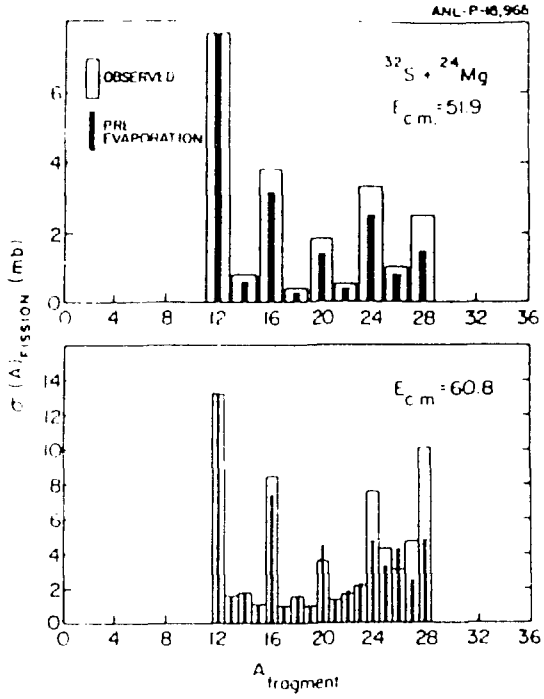

Figure 2. Observed mass distribution (open histograms) and the corresponding deduced pre-evaporation mass distributions (solid histograms) for the fission component of the $^{32}S+^{24}Mg$ reaction at $E_{c.m.}$=51.9 and 60.8 MeV, respectively.

It is clear that after the correction for secondary particle emission is applied, there remains little, if any, memory of the entrance channel in these distributions. Rather, the data suggest purely asymmetric mass distributions. These results are in direct contradiction with any deep-inelastic, "orbiting" picture which views orbiting as an entrance-channel phenomenon.

In the coincidence geometry the experiment is insensitive to ^{8}Be decay since these fragments will immediately break up into two α-particles. However it is possible to obtain an estimate of the ^{8}Be cross

sections, albeit without the coincident detection of the recoiling fragment, using the seven, closely spaced Si (surface barrier) detectors arrayed behind the back proportional counter. The two-alpha hit pattern for these detectors at E_{cm}=51.9 MeV is shown in Fig. 3 by the solid bars.

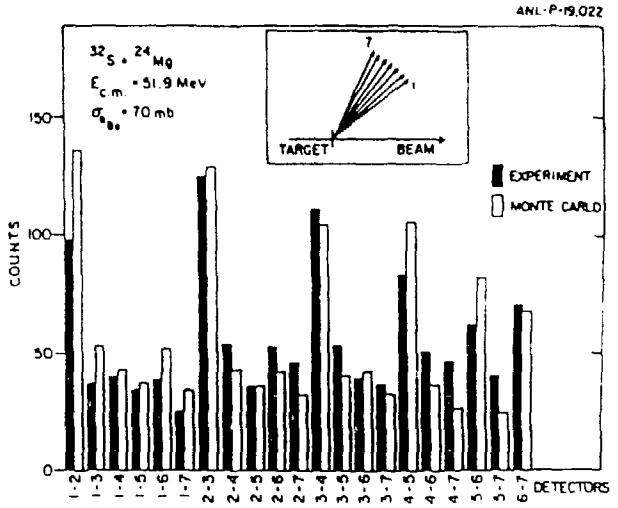

Figure 3. Experimental (solid histograms) and simulated (open histograms) "hit" patterns for the detection of two coincident α-particles from ^8Be decay.

The open bars show the result of a Monte Carlo simulation where it was assumed that the energy and angular distributions of the ^{8}Be fragments follow the same general behavior as found for the heavier mass fragments. A mixture of ground state and first-excited state ^{8}Be population is assumed with the relative proportion set by the simulation of the hit pattern and the observed sum-energy spectra. The greater frequency of finding coincident alpha particles in adjacent detectors can be understood in terms of the maximum opening angle for the decay of ^{8}Be in its ground state—at the energies found in this experiment and for our experimental angular acceptance, only adjacent detectors can be struck for ground state ^{8}Be decays. From this analysis ^{8}Be cross sections of $\sigma(^8Be)$ = 70 mb at $E_{c.m.}$=51.9 MeV and 100 mb at $E_{c.m.}$=60.8 MeV are deduced.

DISCLAIMER

This report was prepared as an account of work sponsored by an agency of the United States Government. Neither the United States Government nor any agency thereof, nor any of their employees, makes any warranty, express or implied, or assumes any legal liability or responsibility for the accuracy, completeness, or usefulness of any information, apparatus, product, or process disclosed, or represents that its use would not infringe privately owned rights. Reference herein to any specific commercial product, process, or service by trade name, trademark, manufacturer, or otherwise does not necessarily constitute or imply its endorsement, recommendation, or favoring by the United States Government or any agency thereof. The views and opinions of authors expressed herein do not necessarily state or reflect those of the United States Government or any agency thereof.

3. STATISTICAL CALCULATION

To see whether these results can be understood in terms of a fusion-fission mechanism it is necessary to first calculate the fission barriers as a function of spin and mass asymmetry for the ^{56}Ni compound nucleus. These calculations, which incorporate diffuse-surface and finite-range effects, were performed following closely the work of Krappe, Davies, Nix, and Sierk[1,11]. The resulting saddle-point energies are shown in Fig. 4.

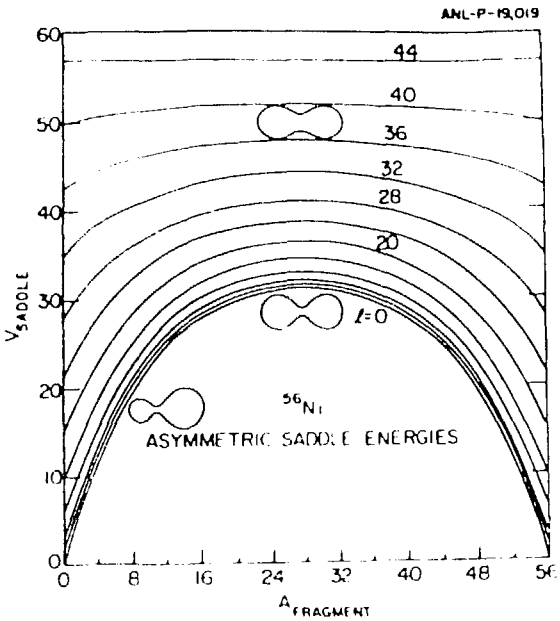

Figure 4. Asymmetric saddle-point energies for the ^{56}Ni compound system. Several of the calculated saddle-point shapes are shown.

For the limiting case of fission to a massless particle the saddle-point energy is taken as the equilibrium energy for ^{56}Ni at the appropriate spin value, as tabulated by Sierk[1]. Some interpolation was necessary between this extreme and the minimum mass asymmetry for which the calculations converged, usually corresponding to a fragment mass of $A_{fragment}$~12. The fission barrier at a given mass asymmetry and spin then corresponds to the difference in energy between the equilibrium value and the corresponding saddle-point energy. From inspection of Fig. 4, one sees that only the higher partial waves are likely to contribute to heavier-mass fission—for the lower partial waves the fission barriers increase rapidly for more symmetric mass channels and no substantial competition can be expected with light-particle evaporation.

The saddle-point energies shown in Fig. 4 have been incorporated into the statistical evaporation code CASCADE[12], where the probability

of fissioning into a given mass partition is assumed to be proportional to the level density above the generalized saddle point (the "ridge" line in Moretto's notation[13]). Since the observed mass distribution shows evidence of shell effects (the cross section for every fourth mass is enhanced), a correction was introduced in the calculation by adjusting the mass-asymmetric, saddle-point energies by a term given by the sum of Wigner energy terms for the two fission fragments. This correction, which does not affect the barrier energies used for the decay to two, even-even nuclei, places an energy penalty against the decay to channels containing even-odd or odd-odd combinations. The results of these calculations are compared with experiment in Fig. 5. (The experimentally derived ^{8}Be cross sections, obtained using a different technique, are not shown, although they would be well off scale.) Reasonable agreement is achieved for $A_{fragment} \gtrsim 12$ using a ratio of the level density parameters for fission as compared to light-particle evaporation of $a_f/a_n = 0.76$. It is interesting to speculate that this observed ratio, indicating a hindrance in the fission channels, may result from the effect of compound-nucleus deformation on the light-particle emission as suggested by Blann[14].

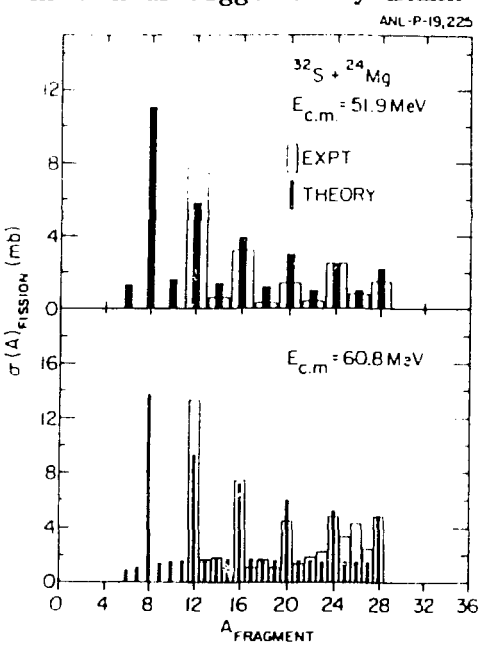

Figure 5. Mass distributions predicted by the Hauser-Feshbach calculation described in the text (solid histograms) compared to the experimental, pre-evaporation mass distributions (open histograms) at $E_{c.m.}$=51.9 and 60.8 MeV, respectively.

The calculated cross sections in the ^{8}Be channel is substantially less than observed. To better understand this, in Fig. 6 the cross sections observed at every fourth mass with $8 \lesssim A_{fragment} \lesssim 28$ are shown as well as

the corresponding CASCADE calculations. The breaks in the calculated curves between mass 4 and 8 correspond to where the calculations change from assuming a post-scission phase space for the light-particle evaporation channels to a saddle-point phase space for fission decay. The ^{8}Be results indicate that this transition region is probably not being properly treated in this model and a more consistent picture placing light-particle evaporation and fission on the same framework is needed. The smooth decline with increasing fragment symmetry suggests a picture where fission and light-particle evaporation are seen as manifesting the same basic physics of statistical compound-nucleus decay.

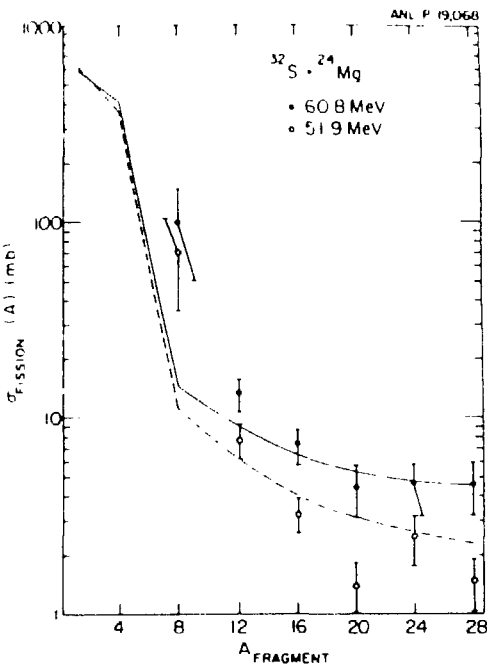

Figure 6. Mass dependence of the cross sections for the stronger fission-decay channels in the $^{32}S+^{24}Mg$ reaction at $E_{c.m.}$=51.9 and 60.8 MeV. The curves indicate the results of the Hauser-Feshbach calculation discussed in the text.

4. DISCUSSION

From the ^{32}S+^{24}Mg measurements substantial fission competition is found even at relatively low energies. If ^{8}Be is included as a fission channel, the total fission cross section for the ^{32}S+^{24}Mg reaction is 90 mb at $E_{c.m.}$= 51.9 MeV and 160 mb at 60.8 MeV, or 9% and 16% of the total fusion cross sections, respectively. (For decay to fragments of mass A≥12, the fission cross sections are 18 mb and 59 mb at the lower and higher energies, respectively.) From the previous discussion of Fig. 4

it is clear that these yields arise from the higher partial waves which contribute to fusion. This is further emphasized in Fig. 7 where the partial wave distributions suggested by the CASCADE calculation for both fusion (solid curve) and fission (dashed curve) are shown, as derived for the $^{32}S+^{24}Mg$ reaction at $E_{c.m.}$=60.8 MeV. Fission decay is seen to dominate above the peak of the fission ℓ distribution at $\ell \simeq 36\hbar$. The grazing angular momentum for this system is around $42\hbar$. It is clear that any discussion of the fusion process in these relatively light systems at higher energies must consider the role of fission, rather than simply equating fusion and evaporation-residue cross section.

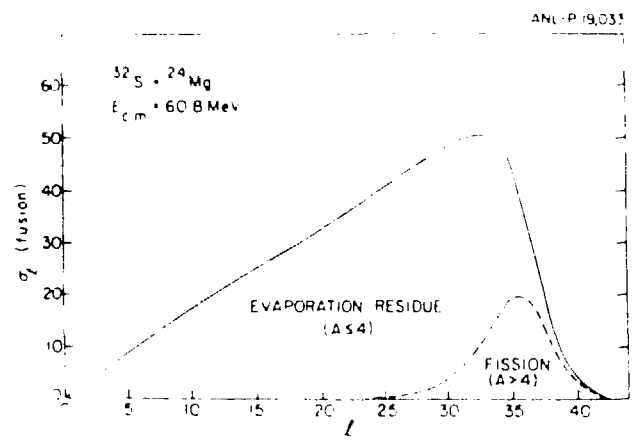

Figure 7. Partial wave distributions for fusion (solid curve) and fission (dashed curve) for the $^{32}S+^{24}Mg$ reaction at $E_{c.m}$=60.8 MeV.

Above a spin value of $44\hbar$ the fission barrier vanishes and the compound nucleus looses all stability against fission decay. This limit on the compound-nucleus spin value may be responsible for the falloff in evaporation-residue cross sections seen in studies of these yields for high-energy $^{16}O+^{40}Ca$ scattering[15-17]. Such a limit should also be manifested as a saturation of the total complete-fusion-fission cross section at higher energies, and some evidence for this has been found in the $^{16}O+^{40}Ca$ system by Beck *et al.*[17] for the more symmetric fission fragments ($20 \leq A \leq 28$). Similar behavior has also been observed in the $^{12}C+^{40}Ca$ system by Grotowski *et al.*[3], although again over a limited mass range. For a conclusive experimental test of the predicted limiting compound-nucleus angular momentum, it will be necessary to carefully unravel the complete fusion and incomplete fusion contributions, where substantial

fission yields are likely to be present in both.

The large ^{8}Be component in the reaction yields has implications for model comparisons with the observed evaporation residue and light particle cross sections. This is seen in Fig. 8 where the measured angular distributions for evaporation-residue cross sections in the three strongest mass channels for the ^{32}S+^{24}Mg reaction at $E_{c.m.}$=60.8 MeV are compared with LILITA calculations (solid curves) which have been scaled to the data. The dashed curves indicate the cross sections which are predicted by LILITA in the A=43 and 46

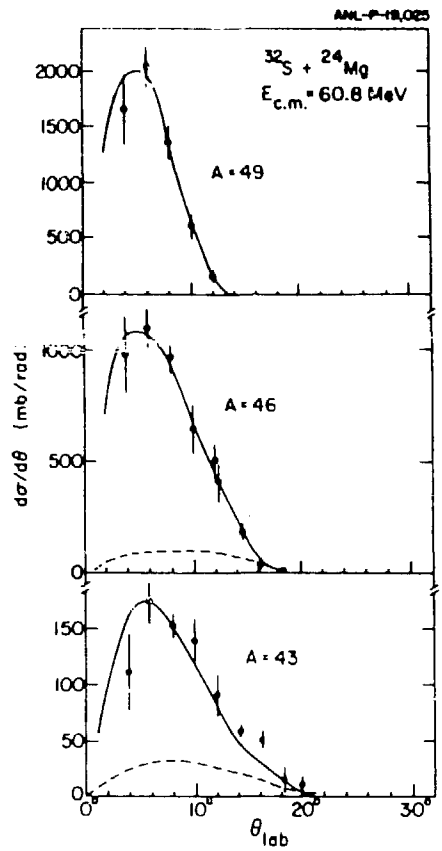

Figure 8. Measured evaporation residue cross sections, and corresponding LILITA predictions (solid curve). The contribution from ^{8}Be decay are indicated by the dashed curves.

channels for the ^{8}Be recoil (^{48}Cr) after secondary light-particle emission and assuming a ^{8}Be cross section of 100 mb. The ^{8}Be contributions are found to peak at larger angles and have broader distributions than for light-particle evaporation. The α-particle spectra should also be influenced by the significantly different kinematics for ^{8}Be decay and α-particle decay. Although the present measurement was not done with sufficient statistics to see these effects, their expected magnitude are sufficiently large as to be seen experimentally. At higher energies, where the evaporation-residue yields shift to lower masses, competition with even heavier-mass, more symmetric fission products should occur.

5. CONCLUSIONS

The fission process is shown to play a significant role in $^{32}S+^{24}Mg$ reactions at energies above 1.5 times the Coulomb barrier. The magnitude and mass asymmetry dependences of the observed fission cross sections are well reproduced by statistical model calculations which include newer estimates for the ^{56}Ni fission barriers, with the fission yields found to originate from the higher fusion partial waves. Since in light systems the fission process favors asymmetric mass channels, both fission and light-particle evaporation residues yields can be expected in some mass channels, although with each showing quite different energy and angular dependences.

I would like to thank my collaborators on this work, including B.B. Back, C. Beck, B.K. Dichter, D. Henderson, R.V.F. Janssens, J.G. Keller, D.G. Kovar, S. Kaufman, T.-F. Wang, B. Wilkins, and F. Videbaek. This work was supported by the U.S. Department of Energy, Nuclear Physics Division, under Contract No. W-31-109-ENG-38.

REFERENCES

1) A.J. Sierk, Phys. Rev. C 33, 2039 (1986).
2) M.A. McMahan *et al.*, Phys. Rev. Lett. 54, 1995 (1985).
3) K. Grotowski *et al.*, Phys. Rev. C 30, 1215 (1984).
4) R. Ritzka *et al.*, Phys. Rev. C 31, 133 (1985).
5) S.J. Sanders *et al.*, Phys. Rev. C 34, 1746 (1986).
6) J. Brzychczyk *et al.*, Phys. Lett. B 194, 473 (1987).
7) R. Moro, *et al.*, Nucl. Phys. A477, 120 (1988).
8) S.J. Sanders *et al.*, Phys. Rev. Lett. 59, 2856 (1987).
9) S.J. Sanders *et al.*, in *Proc. of the Symp. on The Many Facets of Heavy-Ion Fusion Reactions*, Argonne National Laboratory Report ANL-PHY-86-1, 577 (1986).
10) J. Gomez del Campo and R.G. Stokstad, *LILITA, a Monte Carlo Statistical Model Code*,, Oak Ridge National Laboratory Tech. Rep. ORNL-TM-7295 (1981).
11) K.T.R. Davies *et al.*, Phys. Rev. C **16**, 1890(1977); J.R. Nix, Nucl. Phys. A130, 241(1969); K.T.R. Davis and J.R. Nix, Phys. Rev. C 14, 1977(1976); K.T.R. Davies, J.R. Nix, and A.J. Sierk, Phys. Rev. C 20, 992(1979); and H.J. Krappe, J.R. Nix, and A.J. Sierk, Phys. Rev. C 20, 992(1979).
12) F. Puhlhofer, Nucl. Phys. A280, 267(1977).
13) L.G. Moretto, Nucl. Phys. A247, 211(1975).
14) M. Blann, Phys. Rev. C 21, 1770(1980).
15) S.E. Vigdor *et al.* Phys. Rev. C 20, 2147 (1979).
16) Y. Chan *et al.* Phys. Rev. C 27, 447 (1983).
17) C. Beck *et al.* submitted to Phys. Rev. C.